An examination of Wen and Yu's formula for predicting the onset of fluidisation

I.A. Gibson[1], C.J. Slim[1], Yaoyao Zheng[2], S.A. Scott[2], J.F. Davidson[1], A.N. Hayhurst[1]*

1. Department of Chemical Engineering and Biotechnology, University of Cambridge, Philippa Fawcett Drive, Cambridge, CB3 0AS, UK.

2. Department of Engineering, University of Cambridge, Trumpington St, Cambridge, CB2 1PZ, UK.

**Corresponding author at*: Department of Chemical Engineering and Biotechnology, University of Cambridge, Philippa Fawcett Drive, Cambridge, CB3 0AS, UK.

E-mail address: anh1000@cam.ac.uk (A.N.Hayhurst)

Abstract

Classical methods (measuring the pressure drop across a bed for different flowrates of air through the bed) were used to determine the superficial velocity for minimum fluidisation, U_{mf}, of sieved particles of alumina. The particles were characterised optically using an instrument (Morphologi G3, Malvern Instruments), which, from pixelated, enlarged photographs, measured the particles' mean diameter, d_p, to be 0.48 ± 0.04 mm and their sphericity, ϕ, to be 0.77 ± 0.09. Values of U_{mf} were measured for the temperature in the electrically heated bed varying from 14 to 920°C. The results were analysed using Ergun's equation; one outcome was that the voidage, ε_{mf}, in an incipiently fluidised bed was found to be related to the particles' sphericity by:

$$\left(1-\varepsilon_{mf}\right) / \ \phi^2 \varepsilon_{mf}^3 \ = \ 12.2 \pm 0.4.$$

The measured U_{mf} were significantly larger than the values predicted by Wen and Yu's equation, if the mean diameter of the particles was taken, as recommended, to be the geometric mean of the upper and lower sieve sizes, used when preparing the particles. Alternatively, the measured values of U_{mf} were over-predicted by Wen and Yu's equation, when using the optically measured mean size of the particles. The best predictions of U_{mf} were made by using the optically measured mean values of both d_p and ϕ, together with Ergun's equation and the above equation coupling ε_{mf} and ϕ. Such a procedure is proposed for estimating U_{mf} in general. No evidence was found for ε_{mf} varying with temperature.

Highlights

Wen and Yu's equation does not reliably predict the gas velocity for minimum fluidisation

Now the onset of fluidisation can be predicted knowing only the particles' size and sphericity

A relation is suggested between the voidage at incipient fluidisation and the particles' sphericity

Graphical Abstract

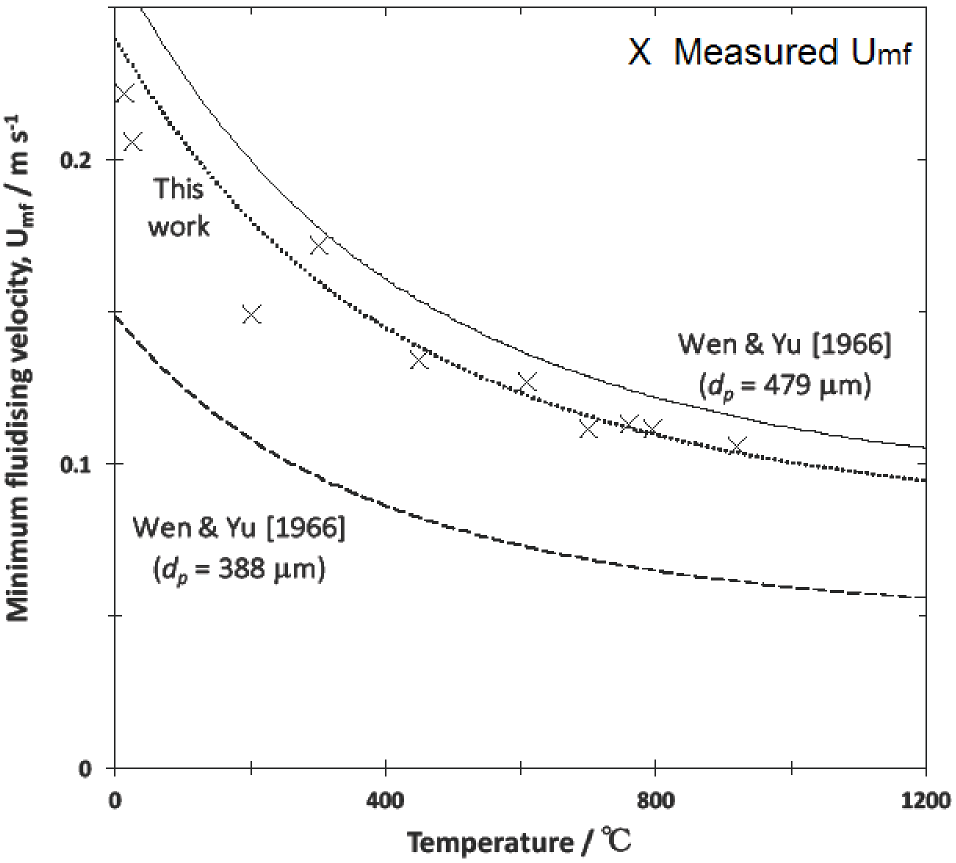

Nomenclature

A_p	The cross-sectional area of a particle's photographic image
c	The circularity of a particle, defined by $(4\pi A_p/L_p^2)$
d_p	The volume-equivalent diameter, *i.e*. the diameter of the sphere with the same volume as the particle under consideration
d_{CE}	The circular equivalent (CE) diameter of a particle, *i.e*. the diameter of the circle with the same area as that of the 2D image of the particular particle
g	The acceleration due to gravity
Ga	The Galileo number $= (\rho_p - \rho_f)\rho_f g d_p^3/\mu^2$
H	The depth of a bed of particles
L_p	The apparent perimeter of a particle as measured from a photograph
Re	The Reynolds number $(\rho_f U_{mf} d_p/\mu)$
S_p	The actual surface area of the particle under consideration

U	The superficial velocity of the gas flowing through a bed of solid particles
U_{mf}	The superficial velocity of the gas at the onset of fluidisation in a bed of solid particles
V_p	The volume of a particle
ΔP	The drop in pressure across a bed of particles, through which air flows
ε	The voidage in a settled bed of solid particles
ε_{mf}	The voidage in a bed at incipient fluidisation
ϕ	The sphericity of a particle, *i.e*. the ratio of the surface area of the sphere with the same volume as the particle to the actual surface area of the particle
μ	The viscosity of the gas flowing through a bed of solid particles
ρ_b	The bulk density of a bed of particles
ρ_f	The density of the air flowing through a bed particles
ρ_p	The density of a particle

1. Introduction

This paper describes simple experiments to check the formula of Wen and Yu (1966), commonly used for predicting U_{mf}, the superficial velocity of the gas for the onset of fluidisation in a bed of solid particles from group B of Geldart's classification (Geldart, 1973). Doubts about Wen and Yu's formula (Eq. (8) below) have been expressed (Botterill, Teoman, 1980, Botterill, Teoman, Yurigir, 1982a, b, Delebarre, 2004, La Nauze, 1986, Howard, 1989), although the equation has proved useful for many practical applications, even at elevated temperatures (Peng Dai, Dennis, Scott, 2016). The experiment described below took a bed of well-characterised particles and measured U_{mf}, when fluidising it with air at temperatures between 14°C and 920°C. Wen and Yu's equation was then assessed in the light of these values of U_{mf}, measured over this wide range of temperature.

2. Experimental

Alumina particles, described below, were fluidised in a stainless steel tube (height 1130 mm, i.d. 78 mm) surrounded by electrical heating coils, operated by a PID controller, using a K-type thermocouple immersed in the bed. A vertical cross-section of the set-up is shown in Fig.1. The bed could be heated to slightly above 1000°C. Fibreglass insulation was packed around the exterior of the heating coils to reduce losses of heat. Laboratory air was passed through the bed (unfluidised depth ~ 250 mm) *via* a stainless steel distributor, which had a square-pitch array of 36 holes (diam. 0.4 mm) around a central tube (stainless steel; i.d. 1.753 mm, o.d. 3.175 mm). This tube protruded above the distributor by ~ 0.5 mm and was used as a pressure-tapping, connected to a water manometer, which measured the difference in pressure across the bed of alumina particles. Control of the flowrate of air was by a needle-valve and rotameter, using flowrates up to 48 l/min, when expressed at room temperature and pressure. The volumetric flowrate at the bed's temperature (measured with the single thermocouple) was calculated using the ideal gas law to account for the elevated temperature inside the bed. The largest source of error arose from the rotameter being unsteady at higher flowrates. Thus above 30 l/min, the rotameter's float oscillated slightly, making it a little more difficult to measure high flowrates of air accurately.

Fig. 1 hereabouts.

Alumina particles were used, chosen for their stability over the temperature range investigated. The particles were washed and sieved to be between 0.355 mm and 0.425 mm, using standard, handheld, laboratory sieves. The bulk density of the unfluidised alumina particles, as well as the density of one particle and the voidage in an unfluidised bed of these particles, were all measured experimentally. To find a particle's density, ρ_p, a known mass of alumina particles was slowly added to a known volume of water in a measuring cylinder. The displacement gave the volume of particles added, thereby yielding a particle's density. The voidage, ε, (the fraction of a settled bed's volume not occupied by particulate matter, but by voids) was estimated by simply measuring the total volume occupied (after some modest shaking inside a wide measuring cylinder) by a known mass (≈ 200 g) of dry particles. Next, the volume of water to reach the top of the particles in the measuring cylinder, *i.e*. the volume of the voids, was measured. Finally, the bulk density, ρ_b, of the particles in a bed was found either directly from the known mass and volume of the particles in the measuring cylinder or by substituting in: $\varepsilon = 1 - \rho_b/\rho_p$. The values measured were: $\rho_b = 2140 \pm 200$ kg/m^3, $\rho_p = 3900 \pm 350$ kg/m^3 and $\varepsilon = 0.45 \pm 0.04$. The geometric mean of the upper and lower sieve sizes was 0.388 mm for a nominal size range of 0.355 – 0.425 mm.

The alumina particles were examined optically using a particle sizer (Morphologi G3; Malvern Instruments), which is a microscope for characterising particles. It estimates their sizes and shapes directly from enlarged photographs, *i.e*. 2D images of 3D particles resting on a microscope slide. Part of the justification of the procedure described below is that errors are minimised, if enough particles are examined, with views from different angles. First, a small cyclone finely dispersed the sample over a microscope slide, thereby minimising the chance of particles touching one another. Microscopy was done both with and without a thin film of cooking oil on the slide to ensure the particles settled in a random way on the slide. The results from both methods were indistinguishable from one another, thereby confirming the absence of a preferred mode for a particle to settle in. The instrument automatically images, pixelates and analyses every particle detected. The operator can also choose to remove manually any *extrema* from the analysis, *e.g.* because of dust particles or particles touching one another. Figure 2 is an image of a few particles; it is clear that they can have extremely sharp points.

Figure 2 hereabouts

The cross-sectional area, A_p, of every particle's pixelated image was measured by the instrument. This then yielded the circular equivalent (CE) diameter, d_{CE}, of each particle; this is the diameter of the circle with the same area as that of the 2D image of the particular particle in *e.g*. Fig. 2. Hence, $d_{CE} = 2\sqrt{(A_p/\pi)}$. Figure 3 shows the fractional volume of 502 particles analysed (selected after thorough mixing), plotted against their circular equivalent (CE) diameter, d_{CE}, in μm. The few smaller particles with d_{CE} less than 300 μm were ignored and attention focused on the particles with $350 < d_{CE} < 580$ μm. Their modal circular equivalent diameter was $d_{CE} = 0.48 \pm 0.04$ mm; this is significantly higher than the geometric mean of the upper and lower sieve sizes, *i.e*. 0.388 mm. In fact, it exceeds the width of the larger sieve, *i.e*. 0.425 mm. Presumably some relatively long and thin particles had passed through the larger sieve.

Figure 3 hereabout

The other measurable quantity from the pixelated images in Fig. 2 is the apparent perimeter, L_p, of each particle. This enables the circularity of the particle to be estimated; this is:

$$c = 4\pi A_p/L_p^2. \qquad (1)$$

The circularity corresponds to the area of the 2D image of a particle divided by $L_p^2/4\pi$. For a sphere, $c = 1$, otherwise, $c < 1$; thus, *e.g*. for a square image of a cube, $c = 0.785$. Figure 4 shows the distribution of the (so called high sensitivity) particles' circularity.

There is a skewed distribution, with the instrument's statistical analysis declaring a most probable value for c of 0.77 ± 0.09. This value of c turns out to be the best available estimate for the sphericity of this sample of particles (Nedderman, 1992). The sphericity, ϕ, of one particle is defined as the ratio of: (the surface area of the sphere with the same volume as the particle) to (the actual surface area of the particle). Mathematically it is:

$$\phi = \frac{\pi^{1/3}\left(6\,V_p\right)^{2/3}}{S_p},$$

whereas the dimensionless circularity, c, was defined in Eq. (1) in terms of A_p and L_p, both of which can be measured from Fig. 2. Again for a sphere, $\phi = 1$. Thus, it has been assumed that good estimates of three-dimensional properties of particles, such as their sphericity, ϕ, can be derived from two-dimensional photographs. Thus in this project, the circular equivalent diameter, d_{CE}, was taken as the best estimate of the surface-volume diameter, d_p, (the diameter of the sphere with the same volume as the particle under consideration), *i.e.* $d_p \approx d_{CE}$. Also, the circularity, c, was assumed to equal the sphericity, ϕ, so $\phi \approx c$. These conclusions were confirmed by the above observation that there was no difference between the observed properties of particles, which had settled on a microscope slide with and without a thin layer of oil. The details of the particles used are summarised in Table 1. The mean value of the particle size, d_p, and the sphericity, ϕ, are important, because they appear again in Ergun's Eq. (2) below.

Figure 4 heareabouts

Table 1. A summary of the parameters used for the particles of alumina.

Geometric Mean of Sieve Sizes	0.388 mm
CE Diameter, $d_{CE} = d_p$	0.48 ± 0.04 mm
Density of a particle, ρ_p	3900 ± 350 kg m^{-3}
Bulk Density. ρ_b	2140 ± 200 kg m^{-3}
Circularity, c (estimate of sphericity, ϕ)	0.77 ± 0.09
Voidage, ε	0.45 ± 0.04

3. Measurement of the Superficial Velocity for Incipient Fluidisation

The cold bed was loaded with a known mass of alumina sand and a small flowrate of air passed through it. Next the bed was heated to the required temperature and then fluidised by increasing the flowrate of air through the bed. The bed was left for a few minutes to allow the temperature to stabilise. Initially the flowrate of gas was well above the minimum for fluidisation. The flowrate of air was then reduced in small steps and readings of the pressure difference across the bed were taken from the manometer. The steps were particularly small around the point of fluidisation to obtain a clear picture of the bed's changing behaviour. This is shown in Fig. 5, which is a plot of the pressure difference across the bed versus the superficial velocity of the air, *i.e.* (the volumetric flow rate of the air at the temperature of the bed) / (cross-sectional area of the bed). Figure 5 is for the bed at 610^{o}C; clearly it has two linear asymptotes. The one through the origin of Fig. 5 is for air flowing through a packed bed; the horizontal one is for when the particles were fully fluidised. In fact, the constant pressure drop across the bed, when fluidised, corresponded at every temperature to the submerged weight of the particles per unit area of the bed, as calculated from the measured mass of all the particles in the bed. This provided a useful check on the position of the horizontal asymptote. The point of intersection of these two asymptotes was used to identify U_{mf}, the value of U for incipient fluidisation. For Fig. 5, this is U_{mf} = 0.127 ± 0.004 m/s measured at 610^{o}C. The error quoted here comes partly from several repeats of Fig. 5.

Figure 5 hereabouts

A quartz tube (i.d. 27.5 mm, with a sintered quartz distributor) housed the particles for investigating the onset of fluidisation for the alumina particles at the two lowest temperatures of 14^{o}C, as on a cold day, and 25^{o}C. This narrow tube was necessary, because the rotameter was too small to provide the high flowrates required to achieve fluidisation at room temperature in the wider, stainless steel, bed. Of course, the pressure drop across the bed was still measured with a manometer. For this a pipe was inserted in the quartz tube, with the open end on the distributor and the other end connected to the manometer. Flowrates of air were again controlled by the needle-valve and rotameter. The quartz tube could not be heated and so was only used at room temperature. At 14^{o}C, because accurate measurements (of the higher flowrates of air) were more difficult to make, use was made of the fact that the horizontal portion of Fig. 5 corresponded to the pressure difference, ΔP, supporting the bed's known weight per unit area. The observations made with the bed at 14^{o}C are shown in Fig. 6, where it will be noticed that the part for low flows of air has been forced very slightly to pass through the origin. The measurements are slightly more scattered than in Fig. 5. Even so, to identify U_{mf} is straightforward. Its value is U_{mf} = 0.221 ± 0.018 m s^{-1}, *i.e.* higher than when the air and particles were at 610^{o}C as in Fig. 5. The error in the U_{mf} measured at 14^{o}C was higher than that derived from Fig. 5 for 610^{o}C.

Fig. 6 hereabouts

4.1 Theory of Incipient Fluidisation.

Many correlations, discussed below, exist for predicting U_{mf}, because there is an obvious advantage in avoiding experiments for measuring U_{mf}. Most models are based on Ergun's equation (Ergun, Orning, 1949; Ergun, 1952; Niven, 2002) for the pressure drop, ΔP, across a packed bed of depth, H:

$$\left(\frac{\Delta P}{H}\right) = 150\frac{(1-\varepsilon)^2\mu U}{\varepsilon^3\phi^2 d_p^2} + 1.75\frac{(1-\varepsilon)}{\varepsilon^3}\frac{\rho_f U^2}{\phi d_p}. \tag{2}$$

This equation was originally for a bed of spherical particles. However, for non-spherical particles, their effective diameter is taken as the mean value of (ϕd_p), where d_p is the diameter of the sphere with the same volume as the particle under consideration (Ergun, Orning, 1949; Ergun, 1952). Wen and Yu (1966) assert that "As an approximation, the particle diameter (*i.e.* d_p) may be calculated from the geometric mean of the two consecutive sieve openings without introducing serious errors". This matter is discussed again below.

The first term on the right-hand side of Eq. (2) represents viscous effects and so is important for low flowrates of air and for small particles, *i.e.* for low Reynolds numbers. The second term is determined by inertial effects and so is for high Reynolds numbers. It must be noted that for non-spherical particles there has been discussion about the precise values of the constants 150 and 1.75 in Eq. (2). Thus alternative values, respectively up to 200 and up to 4.0 have been proposed for these two constants (Leva, 1947; MacDonald *et al*., 1979; Niven, 2002; Ozahi *et al*., 2008). The question of the exact values is discussed again below in the light of experimental measurements.

At minimum fluidisation, the effective weight of the bed must be balanced by the pressure drop across the bed, so:

$$\frac{\Delta P}{H} = (1-\varepsilon)(\rho_p - \rho_f)g\,. \tag{3}$$

Combining Eqs. (2) and (3), for the pressure gradient at the point of incipient fluidisation yields:

$$\frac{(\rho_p-\rho_f)\rho_f g d_p^3}{\mu^2} = \frac{150(1-\varepsilon_{mf})}{\phi^2\varepsilon_{mf}^3}\left(\frac{\rho U_{mf} d_p}{\mu}\right) + \frac{1.75}{\phi\varepsilon_{mf}^3}\left(\frac{\rho_f U_{mf} d_p}{\mu}\right)^2, \tag{4}$$

when $U = U_{mf}$ and $\varepsilon = \varepsilon_{mf}$. In a bed on the point of being fluidised, ε_{mf} is usually slightly larger than ε for a packed bed (Kunii, Levenspiel, 1969). Thus, after defining the dimensionless groups:

$$\mathrm{Ga} = \frac{(\rho_p - \rho_f)\rho_f g d_p^3}{\mu^2} \text{ and } \mathrm{Re} = \left(\frac{\rho_f U_{mf} d_p}{\mu}\right), \tag{5}$$

there results the equation:

$$\mathrm{Ga} = 150\,\frac{(1-\varepsilon_{mf})}{\phi^2\,\varepsilon_{mf}^3}\,\mathrm{Re_{mf}} + \frac{1.75}{\phi\varepsilon_{mf}^3}\,\mathrm{Re_{mf}^2}\,, \tag{6}$$

relating the Galileo and Reynolds numbers. Of course, if quite unusually the diameter, d_p, the sphericity of the particles, ϕ, and the voidage at incipient fluidisation, ε_{mf}, are all known, Eq. (6) could be solved to give the Reynolds number, $\mathrm{Re_{mf}}$ (based on the diameter of the particles), and hence also yield a value for the superficial velocity, U_{mf}, for incipient fluidisation. However, as seen above, it is not at all straightforward to obtain accurate values of these parameters, d_p, ϕ and ε_{mf}. Thus, just one problem is exactly what the value of d_p might be, because in this study the geometric mean of the relevant sieve sizes was 0.388 mm, but the value measured optically (see Table 1) for d_p was 0.48 ± 0.04 mm.

To cope with the usual lack of measured values for the sphericity, ϕ, and ε_{mf}, Wen and Yu (1966) assigned values to the two groups containing these parameters in Eq. (4), as follows:

$$\frac{(1-\varepsilon_{mf})}{\phi^2\,\varepsilon_{mf}^3} \approx 11; \quad \frac{1}{\phi\varepsilon_{mf}^3} \approx 14. \tag{7}$$

For this they used information from both their experiments and the literature; one result of using Eqs. (7) with Eq. (4) is Wen and Yu's correlation (1966), which can be written as:

$$Re_{\mathrm{mf}} = \sqrt{(33.7)^2 + 0.0408\,\mathrm{Ga}} - 33.7. \tag{8}$$

Often this is reasonably accurate at room temperature, so it has been widely used (Yates, 1983, Peng Dai, Dennis, Scott, 2016). It should be stressed that the two simultaneous Eqs. (7) have only one acceptable root of $\phi = 0.67$ and $\varepsilon_{mf} = 0.47$, so that, strictly speaking, Eq. (8), *i.e*. Wen and Yu's correlation, is really only true, when $\phi = 0.67$ and $\varepsilon_{mf} = 0.47$. Such a value for ε_{mf} is sometimes too high (Botterill, 1975), although both ϕ and ε_{mf} do have a variety of values for different particles. Thus, Kunii and Levenspiel (1969) give values of ε_{mf} lying between ~ 0.4 and 0.7 and ϕ between 0.50 and 0.85. This alone brings the universal applicability of Wen and Yu's Eq. (8) into doubt. The approximate values indicated here in Table 1 for the alumina particles under investigation were $\phi = 0.77$ and $\varepsilon = 0.45$ in a settled bed, with the expectation that ε_{mf} is slightly larger than ε. Thus, strictly speaking, one might not expect Wen and Yu's correlation (1966) to hold for these particles of alumina, because ϕ is larger than 0.67, assumed by Wen and Yu (1966) in deriving Eqs. (7) and (8). Also, the point has been made by Narsimhan (1965) and

Delebarre (2004) that ϕ and ε_{mf} are not independent, because the magnitude of ε_{mf} is probably determined by the value of ϕ for a given set of particles. It thus seems that, because Wen and Yu's two Eqs (7) over-stipulate the prediction of U_{mf}, it would be preferable to have only one equation in place of Eqs (7) and also rely on measuring one more quantity, either ε_{mf} or ϕ. Such an approach is adopted below; it might provide more accurate predictions of U_{mf} than by assuming universal values of $\phi = 0.67$ and $\varepsilon_{mf} = 0.47$, as suggested by Wen and Yu (1966).

At this stage it is worth noting that *inter alia* Saxena and Vogel (1977) offered their own values of the constants in Eq. (7); they prefer $(1 - \varepsilon_{mf})/\phi^2 \varepsilon_{mf}^3 = 5.9 \pm 0.6$ and $1/\phi\varepsilon_{mf}^3 = 10.0 \pm 0.4$, somewhat different from Eq. (7). These two simultaneous equations have one realistic solution $\phi = 0.87$ and $\varepsilon_{mf} = 0.49$. It is interesting that Saxena and Vogel's experiments (1977) involved temperatures up to 430°C and pressures from 179 to 834 Pa. Other alternatives to Eqs (7) are discussed below after the values of U_{mf}, measured here over an unusually wide range of temperatures, have been considered.

4.2 Plotting (Ga/Re_{mf}) against Re_{mf}

Equation (6) can be rearranged to:

$$\left(\frac{\mathrm{Ga}}{\mathrm{Re_{mf}}}\right) = 150\,\frac{(1-\varepsilon_{mf})}{\phi^2\,\varepsilon_{mf}^3} + \frac{1.75}{\phi\varepsilon_{mf}^3}\mathrm{Re_{mf}}. \tag{9}$$

Hence, a plot of $(\mathrm{Ga}/\mathrm{Re_{mf}})$ against $\mathrm{Re_{mf}}$ should yield a straight line, whose slope and intercept are characterised by the sphericity, ϕ, and voidage, ε_{mf}, properties which are assumed *pro tem* not to vary with the temperature of the bed. Figure 7 shows such a plot, using the U_{mf} measured here, together with the values of d_p determined optically and also values of μ and ρ_f for the temperature of the fluidising air. The best fit line certainly has the expected shape with a clear slope and intercept for Re_{mf} up to 7.2.

Fig. 7 hereabouts

The slope and intercept of the regression line in Fig. 7 were measured to be, respectively:

$$\frac{1.75}{\phi\varepsilon_{mf}^3} = 61 \pm 20; \quad 150\,\frac{(1-\varepsilon_{mf})}{\phi^2\,\varepsilon_{mf}^3} = 1837 \pm 63. \tag{10}$$

Thus the intercept, corresponding to observations made at low Re_{mf}, *i.e*. at high temperatures, was measured much more accurately than the slope. The intercept in Fig. 7 indicates that:

$$\frac{(1-\varepsilon_{mf})}{\phi^2\,\varepsilon_{mf}^3} = 12.2 \pm 0.4. \tag{11}$$

This compares fairly well with the value of ≈ 11, assumed in Wen and Yu's (1966) Eq. (7), but less well with the value of 5.9 ± 0.6 favoured by Saxena and Vogel (1977). However, the slope of the best fit line in Fig. 7, which, of course, is particularly sensitive to the measurements at high Re_{mf}, suggests $1/\phi\varepsilon_{mf}^3$ = 35 ± 11. This is 2.5 times larger than Wen and Yu's value of 14 in Eq. (7) and 3.5 times bigger than Saxena and Vogel's (1977) value of 10.0 ± 0.4. That both the slope and intercept of the best-fit line in Fig. 7 are slightly higher than expected could result from the two numerical constants in Eq. (2) not being exactly 150 and 1.75, as noted above. Together, the slope and intercept as presented in Eq. (10) indicate $\varepsilon_{mf} \approx 0.24$ and $\phi \approx 2.1$. These unacceptable values imply that it is extremely difficult to deduce say ε_{mf}, because of the problem of measuring accurately the slope of Fig. 7, which has a small range of Re_{mf} up to 7.2. However, one important conclusion is that the intercept in Fig. 7 (corresponding to measurements made at low Re_{mf}, *i.e.* high temperatures) can be measured quite accurately, in fact to within 4 %. This leads to Eq. (11), which clarifies how the voidage at incipient fluidisation, ε_{mf}, depends on the sphericity, ϕ, for the particles under consideration. Equation (11) holds well for beds at elevated temperatures. Interestingly the value of ϕ = 0.77 ± 0.09 measured optically here, when substituted in Eq. (11) yields ε_{mf} = 0.43. This value is very much what might have been expected. Then assuming ϕ = 0.77 and ε_{mf} = 0.43 leads to $1/\phi\varepsilon_{mf}^3$ = 16.3, instead of ≈ 14, as suggested by Wen and Yu (1966) in Eq. (7). Equation (11) slightly re-writes one of the two Eqs. (7) of Wen and Yu (1966) and because of its apparent accuracy will be taken seriously as relating ϕ to ε_{mf}. It might be noted that Eq. (11) with ϕ = 1 for uniform spheres gives ε_{mf} = 0.39. This lies between the values of ε = 0.48 for closely packed uniform spheres in a cubic lattice and ε_{mf} = 0.32 in a body-centred-cubic structure (Atkins, 1986). This value of ε_{mf} = 0.39 is accordingly plausible for uniform spheres, confirming Eq. (11).

The measured values of U_{mf} are compared in Fig. 8 with various predictions. It is striking that Wen and Yu's correlation, Eq. (8), seriously under-predicts U_{mf}, if the mean value of d_p is taken to be the geometric mean of the upper and lower sieve sizes, previously used by other authors, including Wen and Yu (1966). This is an important conclusion, that Wen and Yu's correlation cannot always be relied upon, if the geometric mean of the two sieve sizes is assumed to be the appropriate value for d_p. On the other hand, Fig. 8 shows that using the value of d_p = 0.479 mm, as measured optically above, together with Wen and Yu's Eq. (8), yields values of U_{mf}, which are slightly too high. As for the other predictions in Fig. 8, the modified Ergun Eq. comes from substituting in Eq. (4) the values of d_p and ϕ measured optically (see Table 1), together with ε_{mf} = 0.45, *i.e.* ε from Table 1. In addition, Fig. 8 includes predictions from an empirical formula:

$$\mathrm{Re_{mf}} = 7.33 \times 10^{-5} \times 10^{\sqrt{(8.24 \log_{10}\mathrm{Ga} \; - \; 8.81)}} ,$$

devised by Wu and Baeyens (1991). These last two correlations give better predictions than Saxena and Vogel's (1977) modification of Wen and Yu's correlation, Eq. (8).

Fig. 8 hereabouts

Very importantly, the preceding discussion provides a new way of predicting U_{mf}. This is to accept Eq. (6), together with the values of ϕ and d_p measured optically, as above. Then ϕ can be substituted in Eq. (11) to yield ε_{mf}. The resulting values of ϕ, ε_{mf} and d_p can then be substituted in Eq. (6) to calculate values of Re_{mf} and thence U_{mf}. The resulting predictions of U_{mf} are shown in Fig. 9 as the dotted line. They are seen to be in good agreement with the measurements. Also included in Fig. 9 for comparison are two curves from Fig. 8, *i.e.* the predictions from Wen and Yu's Eq. (8) using for d_p either the value measured optically here or the geometric mean of the two sieve sizes. The U_{mf} predicted by our proposed method, based on the optically measured d_p and ϕ, are better than the other predictions.

Fig. 9 hereabouts

5. Discussion

It was mentioned above that alternative constants for the right hand side of Eqs (7) have been determined previously. Some such values are collected in Table 2; several of them originate from the excellent review by Lettieri and Macri (2016). Interestingly the means and standard deviations of the values listed in Table 2 are:

$$\left(1-\varepsilon_{mf}\right) / \; \phi^2 \varepsilon_{mf}^3 \; = \; 8.8 \pm 2.4, \tag{12}$$

$$1 \, / \, \phi \varepsilon_{mf}^3 \; = 13.0 \pm 2.5.$$

However, the values in Table 2 refer to solids with a wide range of sizes, shapes and densities. Even so, the above value of $\left(1-\varepsilon_{mf}\right) / \; \phi^2 \varepsilon_{mf}^3 \; = \; 12.2 \pm 0.4$, in Eq. (11) and deduced from Fig. 7 is within the range of values listed in Table 2, if the errors of the data in Table 2 are included.

Table 2. Literature values of the two constants on the right-hand side of Eqs (7)

Reference	$(1-\varepsilon_{mf})\ /\ \phi^2 \varepsilon_{mf}^3$	$1\ /\ \phi\varepsilon_{mf}^3$
Wen & Yu (1966)	11.0	14.0
Bourgeois & Grenier (1968)	8.9	14.9
Saxena & Vogel (1977)	5.9	10.0
Babu *et al.* (1978)	5.2	8.8
Richardson & Jeronimo (1979)	9.4	15.7
Grace (1982)	8.9	14.0
Chitester & Kornosky (1984)	7.7	11.6
Thonglimp *et al.* (1984)	9.9	13.4
Nakamura *et al.* (1985)	9.7	12.3
Lucas & Arnaldos (1986)	5.0	8.5
Adánaz & Abanades (1991)	9.0	15.3
Bin (1993)	9.4	14.8
Reina *et al.* (2000)	14.2	12.7
Zhu *et al.* (2007)	8.3	16.1

The real situation appears to be more complex than the physics behind both the Ergun Eq. (2) and Wen and Yu's correlations, Eqs (7) and (8). In fact, the literature on the topic is complex and by no means agreed upon, so the proposed procedure of predicting U_{mf} using Eqs (6) and (11), together with optically measured values of ϕ and d_p, seems simple, useful and promising. The main factors missing from Eqs (2) and (7) were first discussed by Botterill *et al.* (1980, 1982a, b, c). Of course, the viscosity, μ, of the fluidising gas increases with temperature, but, as was done here, that can be allowed for. Thus, changes in ρ_f and μ affect exactly how the hydrodynamic forces on fluidised particles vary with temperature. However, Botterill *et al.* (1980, 1982a, b), as well as Lucas *et al*. (1986) and Saxena *et al.* (1987) have concluded that, in the laminar flow regime for Geldart's group B particles, ε_{mf} varies with temperature. Thus on raising the temperature above its ambient value, they report that ε_{mf} can initially fall and subsequently increase. Also, according to Lucas *et al*. (1986), there can be changes of ε_{mf} with Re_{mf}, because the boundary layer around each fluidised particle changes with Re_{mf}, so the mean distance between adjacent particles, and consequently

ε_{mf}, also varies. Forces between neighbouring particles can be important, when the particles are small. Apparently the effect of these forces can be altered by changing the temperature (Lettieri, Macri, 2016). Thus Lin *et al.* (2002) after fluidising silica particles concluded that inter-particle forces might well vary with temperature and so affect ε_{mf}. Such forces are difficult to assess on an *a priori* basis.

With reference to the previous paragraph, it must be mentioned that Pattipati and Wen (1981, 1982) reached the conclusion that ε_{mf} definitely does not vary with temperature. However, when considering the effect of temperature on ε_{mf}, Saxena and Vogel (1977), as well as Wu and Baeyens (1991), decided that ε_{mf} can sometimes be taken to be constant. In this context, it is important to ascertain whether the measurements here of U_{mf} from 14 to 920°C provide any evidence for (or against) ε_{mf} increasing with temperature. The intercept in Fig. 7 for Re $\rightarrow$ 0 is sensitive to ε_{mf}, because it is proportional to $\left(1-\varepsilon_{mf}\right) / \phi^2 \varepsilon_{mf}^3$. The intercept refers mainly to measurements at high temperatures and yet its value is well-defined in Fig. 7. Also, the slope of the best-fit line is constant, although its magnitude is possibly higher than expected. It equals: $1 / \phi\varepsilon_{mf}^3 = 35 \pm 11$ and consequently is very dependent on ε_{mf}.. Such a steep, constant slope might originate in uncertainties in the numerical constants in Eq. (2), as noted above; its large error is probably due to the limited range of Re_{mf} explored experimentally in Fig. 7. Even so, overall there is no strong evidence from Fig. 7 that ε_{mf} varies systematically with temperature for the alumina particles investigated here from 14 to 920°C. Further work is however needed, particularly using a wider variety of particles.

6. Conclusions

Washed particles of alumina were sieved to be between 355 μm and 425 μm; their mean diameter, d_p, and sphericity, ϕ, were measured optically. Beds of these particles were fluidised by air at atmospheric pressure and temperatures from 14°C to 920°C, to enable U_{mf} to be measured over this range of temperature. Wen and Yu's correlation, Eq. (8), was found to seriously under-estimate all these measured U_{mf}, if d_p was assumed to be the geometric mean of the sizes of the upper and lower sieves used to select the particles. If the considerably larger value of d_p was used from the optical measurements of d_p, Wen and Yu's correlation slightly over-predicted U_{mf}. These facts highlight the problem of what is the appropriate mean diameter, with which to characterise the particles. Analysis of the measurements of U_{mf}, coupled with the optically measured d_p indicated that

$$\left(1-\varepsilon_{mf}\right) / \ \phi^2 \varepsilon_{mf}^3 \ = \ 12.2 \pm 0.4, \tag{11}$$

i.e. a relation, which couples the sphericity, ϕ, with the voidage, ε_{mf}, at incipient fluidisation. This equality was used, together with the values of both d_p and ϕ, measured optically, as well as Ergun's Eq. (2), to estimate U_{mf} at temperatures between 14 and 920°C. The agreement between the measured U_{mf} and these predictions was good, so it is suggested that here is a better way of estimating U_{mf} than relying on Wen and Yu's correlation and only one measurement, *i.e.* of d_p. Such an approach avoids the difficulty that Wen and Yu's equation is, strictly speaking, only true if ε_{mf} = 0.47 and ϕ = 0.67. No evidence was found for ε_{mf} varying with temperature.

Acknowledgement

We are grateful to Mr Z.S. Saracevic for help characterising the particles.

References

Adánaz, J., Abanades, J.C., 1991, Minimum fluidization velocities of fluidized-bed coal-combustion solids, Powder Technol., 67, 113 – 119.

Atkins, P.W., 1986, Physical Chemistry, 3rd Ed., Oxford University Press, Oxford, p. 567.

Babu, S.P., Shah, B., Talwalker, A., 1978, Fluidization correlations for coal gasification materials – minimum fluidization velocity and fluidized bed expansion ratio, AIChE Symp. Ser, 176 – 186.

Bin, A.K., 1993, Prediction of the minimum fluidization velocity, Powder Technol., 81, 197 – 199.

Botterill, J.S.M., 1975, Fluid-bed heat transfer, Academic Press, London, p. 72.

Botterill, J.S.M., Teoman, Y., 1980, Fluid bed behaviour at elevated temperatures, Fluidization, Eds J.R. Grace, J.M. Matsen, Plenum, New York, 1980, 93 – 100.

Botterill, J.S.M., Teoman, Y, Yüregir, K.R., 1982a, The effect of operating temperature on the velocity of minimum fluidization, bed voidage and general behaviour, Powder Technol., 31, 101 – 110.

Botterill, J.S.M., Teoman, Y, Yüregir, K.R., 1982b, The effect of temperature on fluidized bed behaviour, Chem. Eng. Comm., 15, 227 – 238.

Botterill, J.S.M., Teoman, Y, Yüregir, K.R., 1982c, Comments on "Minimum fluidization velocity at high temperatures", Ind. Eng. Chem., Process Des. Dev., 21, 784 – 785.

Bourgeois, P., Grenier, P., 1968, The ratio of terminal velocity to minimum fluidising velocity for spherical particles, Can. J. Chem., 46, 325 – 328.

Chitester, D., Kornosky, R., 1984, Characteristics of fluidization at high pressure, Chem. Eng. Sci., 39, 253 – 261.

Delebarre, A., 2004, Revisiting the Wen and Yu equation for minimum fluidization velocity, Chem Eng. Res Des., 82, 587 – 590.

Ergun, S., 1952, Flow through packed columns, Chem. Eng. Prog., 48, 89 – 94.

Ergun, S., Orning, A.A., 1949, Fluid flow through randomly packed columns and fluidized beds, Ind. Eng. Chem., 41,1179 – 1184.

Geldart, D., 1973, Types of gas fluidization, Powder Technol., 7, 285 - 292.

Grace, J.R., 1982, Handbook of multiphase systems, Ed. Hetsroni, G., McGraw-Hill, New York, Chapter 8.1.

Howard, J.R., 1989, Fluidized bed technology, principles and applications, Adam Hilger, Bristol, p. 32.

Kunii, D., Levenspiel, O., 1969, Fluidization Engineering, Krieger, Florida.

La Nauze, R.D., 1986, Combustion in fluidized beds, Advanced Combustion Methods, Ed. F.J. Weinberg, Academic Press, London, 17 – 111.

Leva. M., 1947, Pressure drop through packed beds, Chem. Eng. Prog., 43, 549 – 554.

Lettieri, P., Macri, D., 2016, Effect of process conditions on fluidization, Kona Powder and Particle J., 33, 86 – 108.

Lin, C.L., Wey, M.Y., You, S.D., 2002, The effect of particle size distributions on minimum fluidization velocity at high temperatures, Powder Technol., 126, 297 – 301.

Lucas, A., Arnaldos, J., 1986, Improved equation for the calculation of minimum fluidization velocity, Ind, Eng. Chem. Proc. Des. Dev. 25, 426 – 429.

Lucas, A., Arnaldos, J., Casal, J., Puigjaner, L., 1986, High temperature incipient fluidization in mono- and polydisperse systems, Chem. Eng. Comm., 41, 121 – 132.

MacDonald, I.F., Al-Sayed, M.S., Mow, K., Dullien, F.A.L., 1979, Flow through porous media – the Ergun equation revisited, Ind. Eng. Chem. Fund., 57, 527 – 534.

Nakamura, M., Hamada, Y., Yoyama, S., Fouda, A.E., Caoes, C.E., 1985, An experimental investigation of minimum fluidization velocity at elevated temperatures and pressures, Can. J. Chem. Eng., 63, 8 – 13.

Narsimhan, G., 1965, On a generalized expression of prediction of minimum fluidization velocity, A.I.Ch.E. J., 11, 550 – 554.

Nedderman, R.M., 1992, Statics and kinematics of granular materials, Cambridge University Press, Cambridge, p. 135.

Niven, R.K., 2002, Physical insight into the Ergun and Wen and Yu equations for fluid flow in packed and fluidized beds, Chem. Eng. Sci., 57, 527 – 534.

Ozahi, E., Gungdogdu, M.Y., Carpinlioglu, M. Ö., 2008, A modification on Ergun's correlation for use in cylindrical packed beds with non-spherical particles, Adv. Powd. Technol., 19, 369 – 381.

Pattipati, R.C., Wen, C.Y., 1981, Minimum fluidization velocity at high temperatures, Ind. Eng. Chem,. Proc. Des. Dev., 20, 705 - 708.

Pattipati, R.C., Wen, C.Y., 1982, Response to "Minimum fluidization velocity at high temperatures", Ind. Eng. Chem,. Proc. Des. Dev., 21, 785 - 786.

Peng Dai, Dennis, J.S., Scott, S.A., 2016, Using an experimentally-determined model of the evolution of pore structure for the gasification of chars by CO_2, Fuel, 171, 29 – 43.

Reina, J., Velo, E., Puigjaner, L., 2000, Predicting the minimum fluidization velocity of polydisperse mixtures of scrap-wood particles, Powder Technol., 111, 245 – 251.

Richardson, J., Jeronimo, M., 1979, Velocity – voidage relations for sedimentation and fluidisation, Chem. Eng. Sci., 5, 1419 – 1422.

Saxena, S.C., Vogel, G.J., 1977, The measurement of incipient fluidisation velocities in a bed of coarse dolomite at temperature and pressure, Trans. I. Chem. E., 55, 184 – 189.

Saxena, S.C.,Mathur, A., Zhang, Z.F., 1987, Incipient fluidization at different temperatures and powder characterization, AIChE. J., 33, 500 - 502.

Thonglimp, V., Hiquily, N., Laguerie, C., 1984, Vitesse minimale de fluidisation et expansion des couches fluidisées par un gaz, Powder Technol., 38, 233 – 253.

Wen, C.Y., Yu Y.H., 1966, A generalized method for predicting the minimum fluidization velocity, AIChE J, 12, 610 – 612.

Wu, S.Y., Baeyens, J., 1991, Effect of operating temperature on minimum fluidization velocity, Powder Technol., 67, 217 – 220.

Yates, J.G., 1983, Fundamentals of fluidized-bed chemical processes, Butterworths, London, p. 9.

Zhu, Z.P., Na, Y.J., Lu, Q.G., 2007, Effect of pressure on minimum fluidization velocity, J. Therm. Sci., 16, 264 – 269.

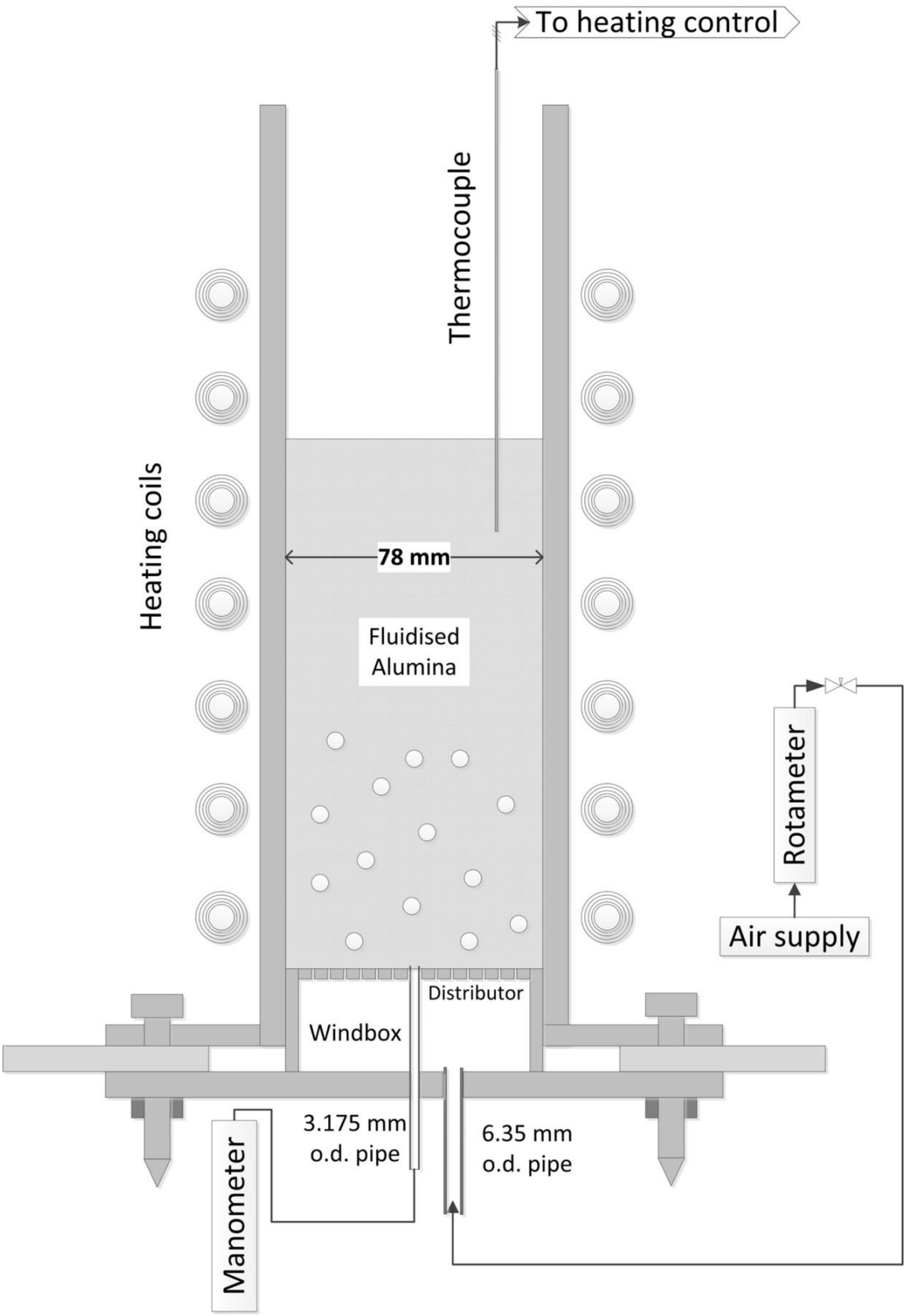

Fig. 1 - A vertical cross-section of the fluidised bed, its windbox and support. The spheres in the bed of particles represent bubbles rising up the bed, when fluidised.

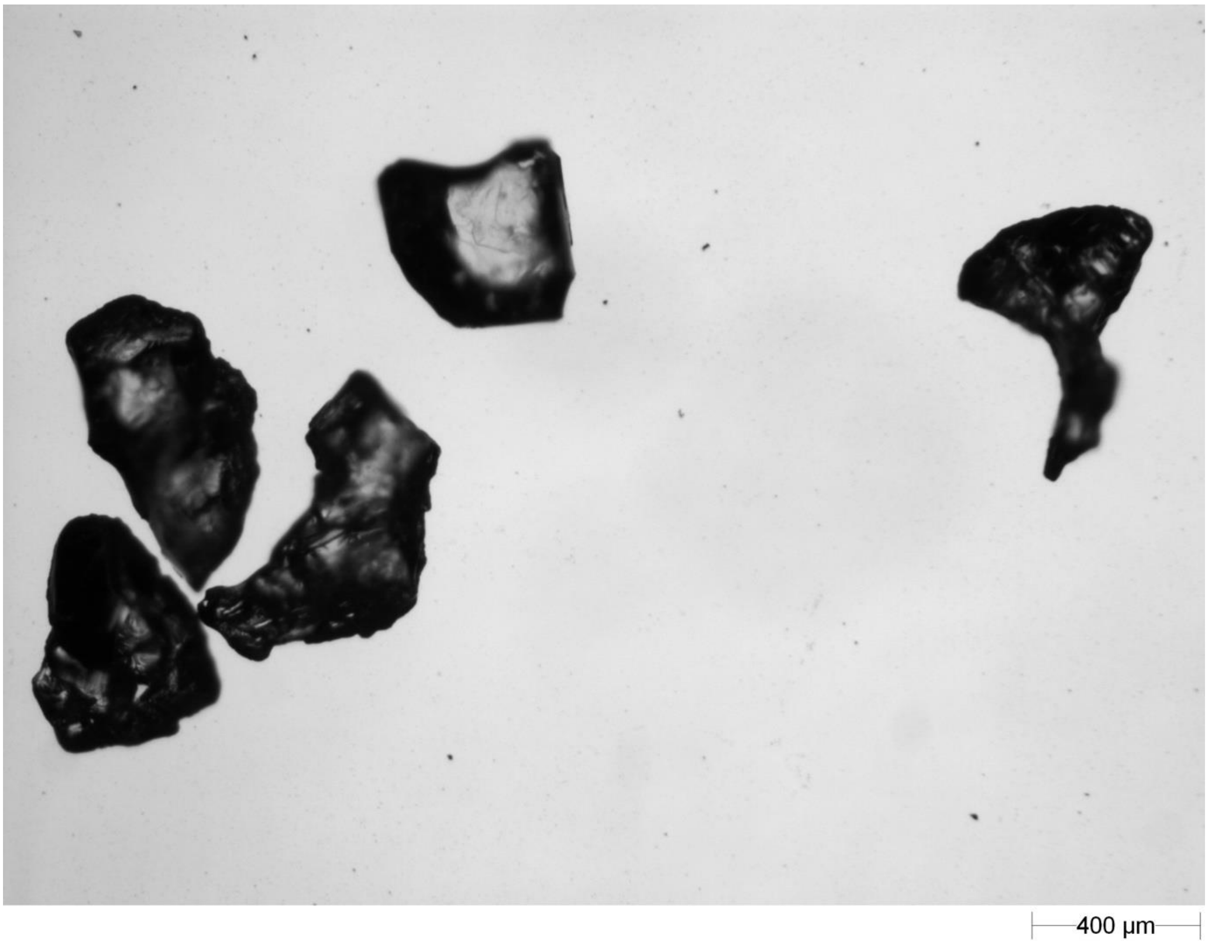

Fig. 2 - Some of the particles of alumina used in this study; the distance for 400 µm is shown.

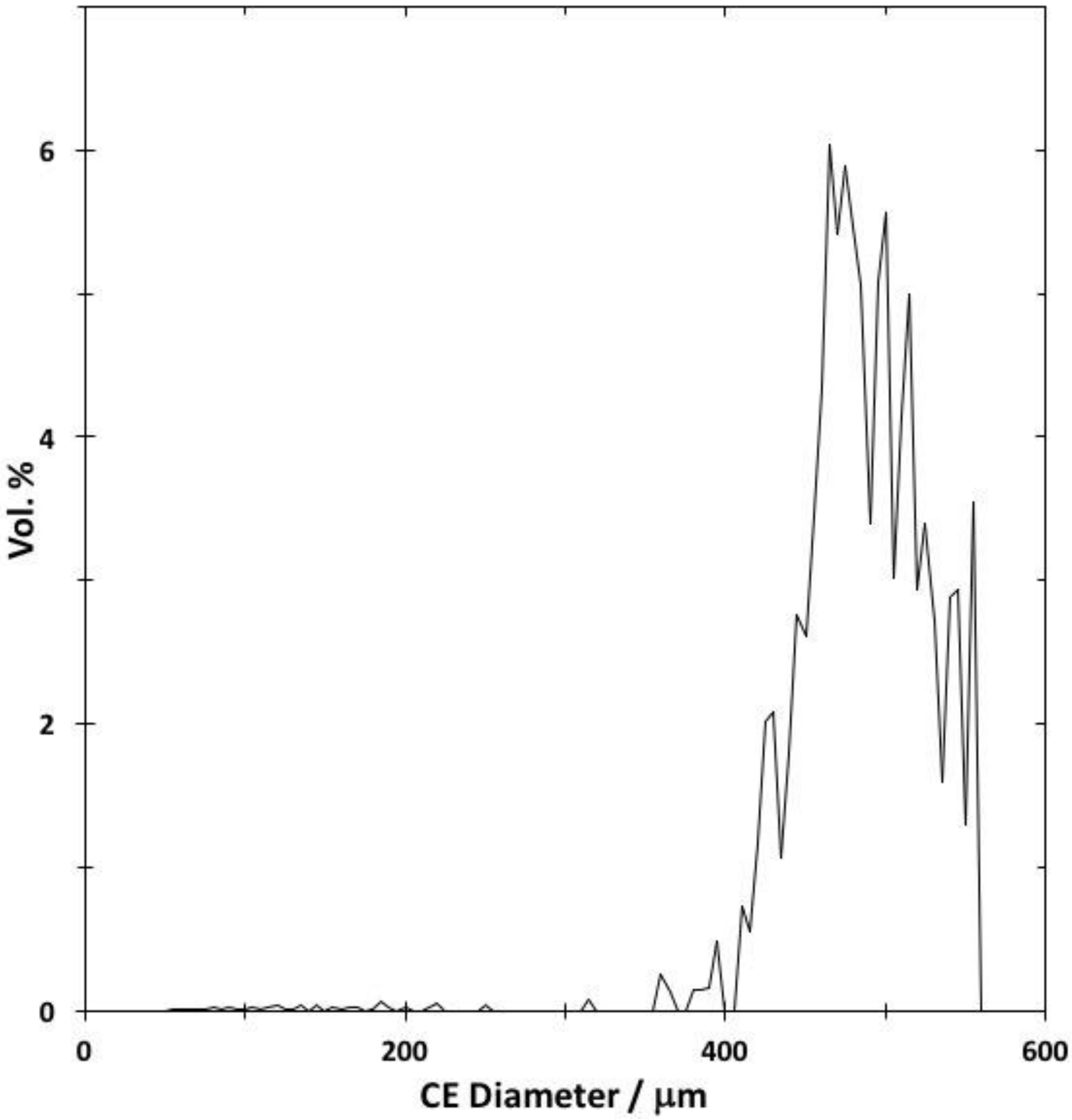

Fig. 3- The measured fraction (of the total volume of the 502 alumina particles studied) having particular (circular equivalent) diameters.

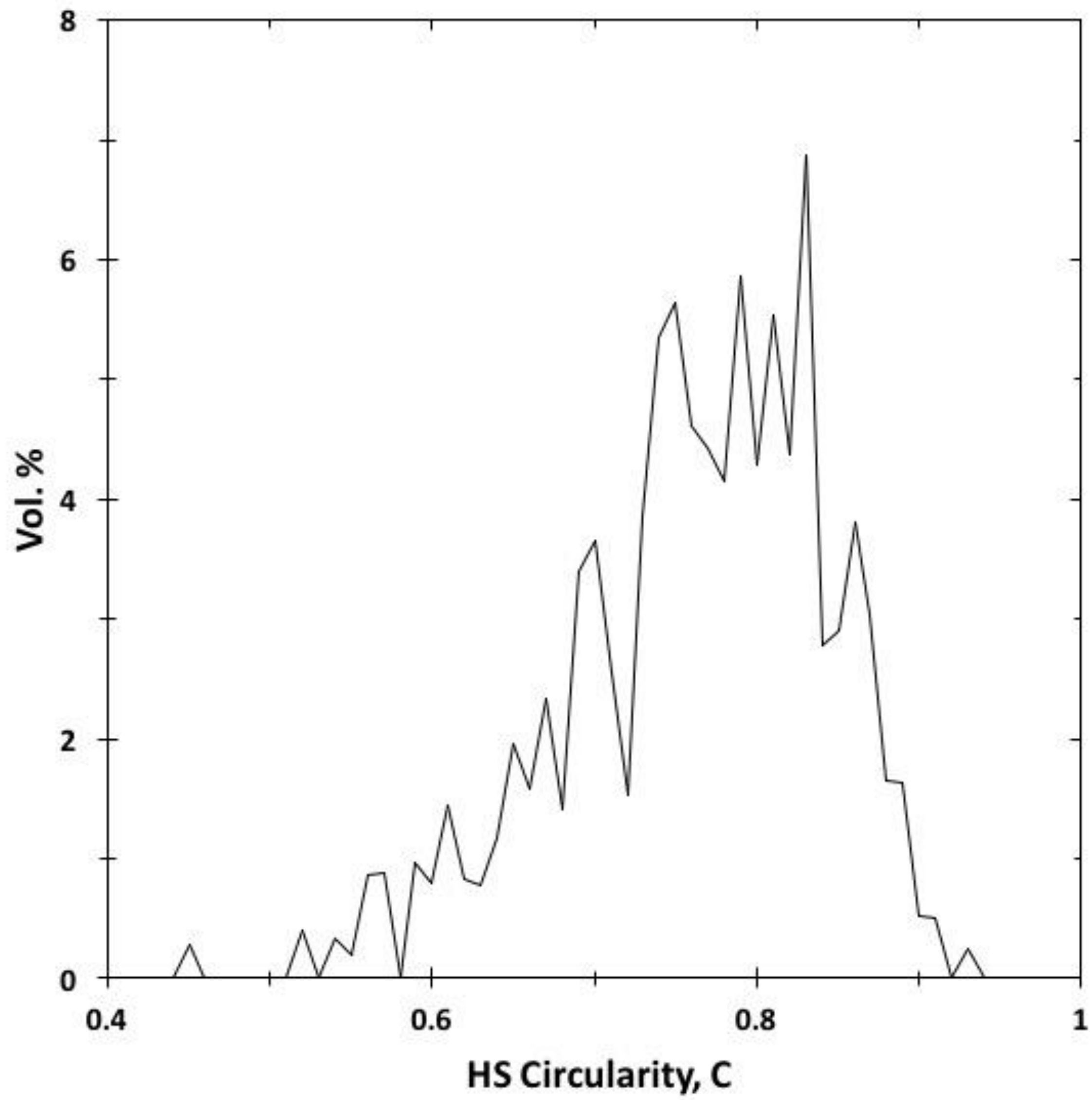

Fig. 4 - The fraction of the total volume of the 502 particles with particular values of the ("high sensitivity") circularity, *c*. The results are for the same particles as in Fig. 3.

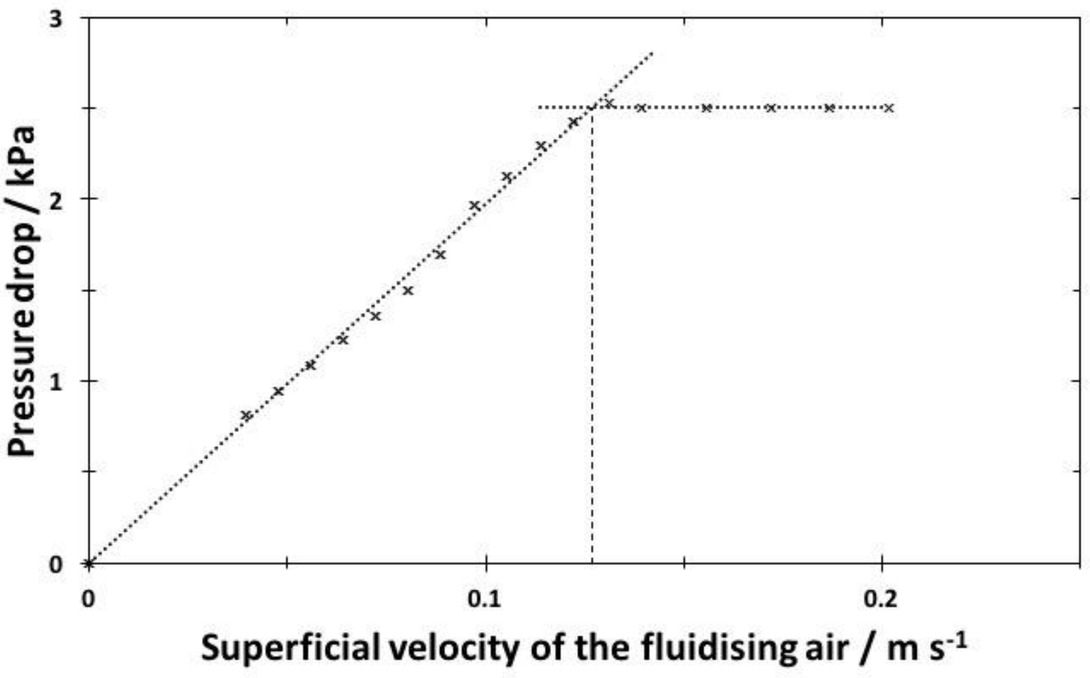

Fig. 5 - A typical plot of the pressure drop, *ΔP,* across the bed against the superficial velocity, *U*, of the air through the bed at 610°C. The vertical broken line gives U_{mf}; defined by the intersection of the other two straight lines.

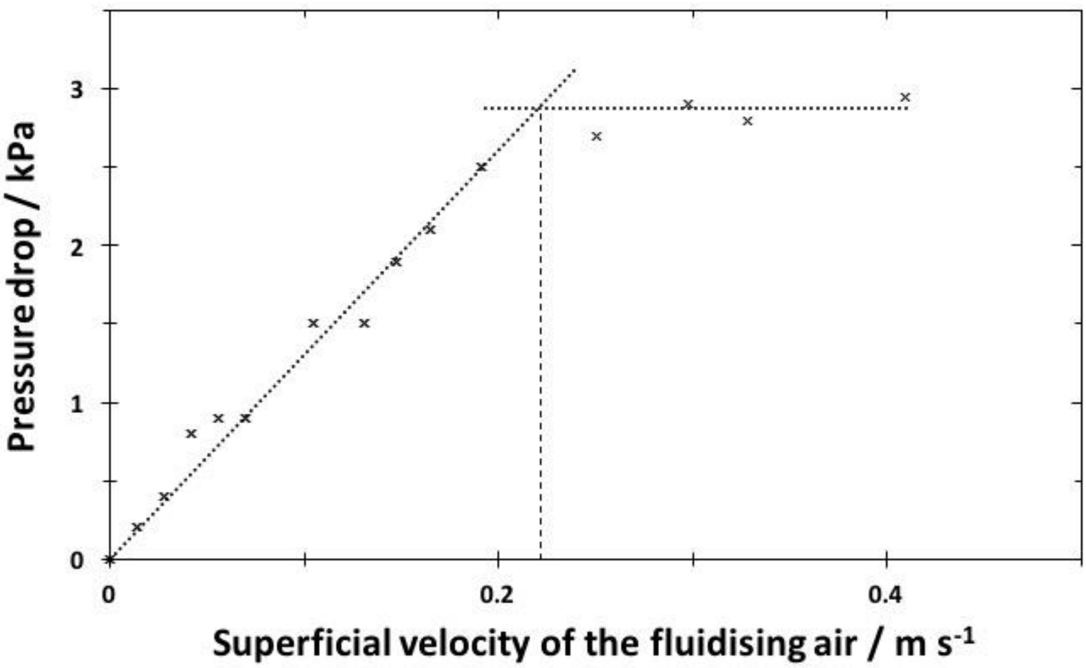

Fig. 6 - Plot of the pressure drop across the bed versus the superficial velocity, U, of the fluidising air at 14ºC.

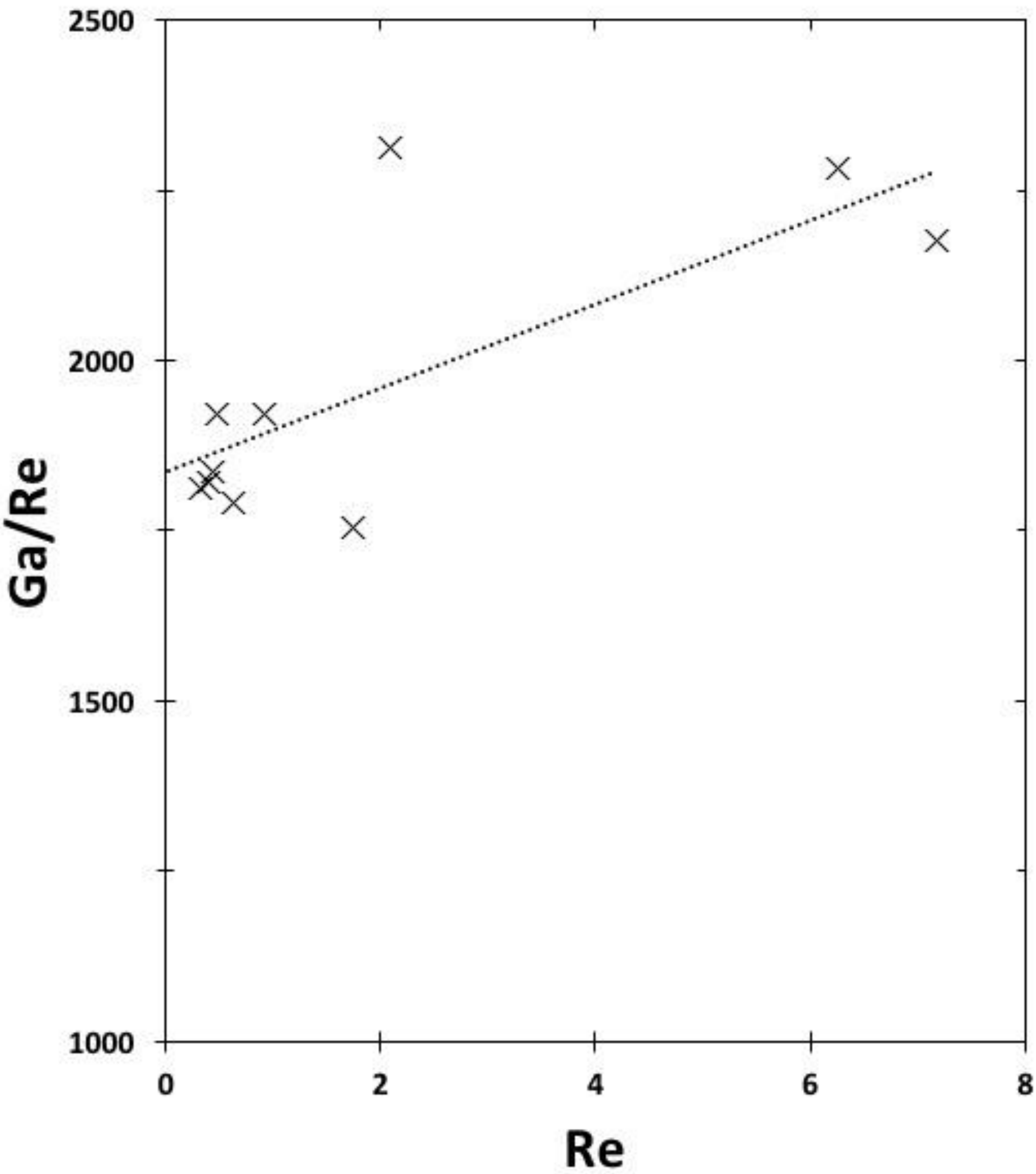

Fig. 7 - Plot of (Ga/Re_{mf}) versus Re_{mf} using the measured values of U_{mf} to check Eq. (9). The best-fit straight line is shown; its slope and intercept are given by Eq. (10).

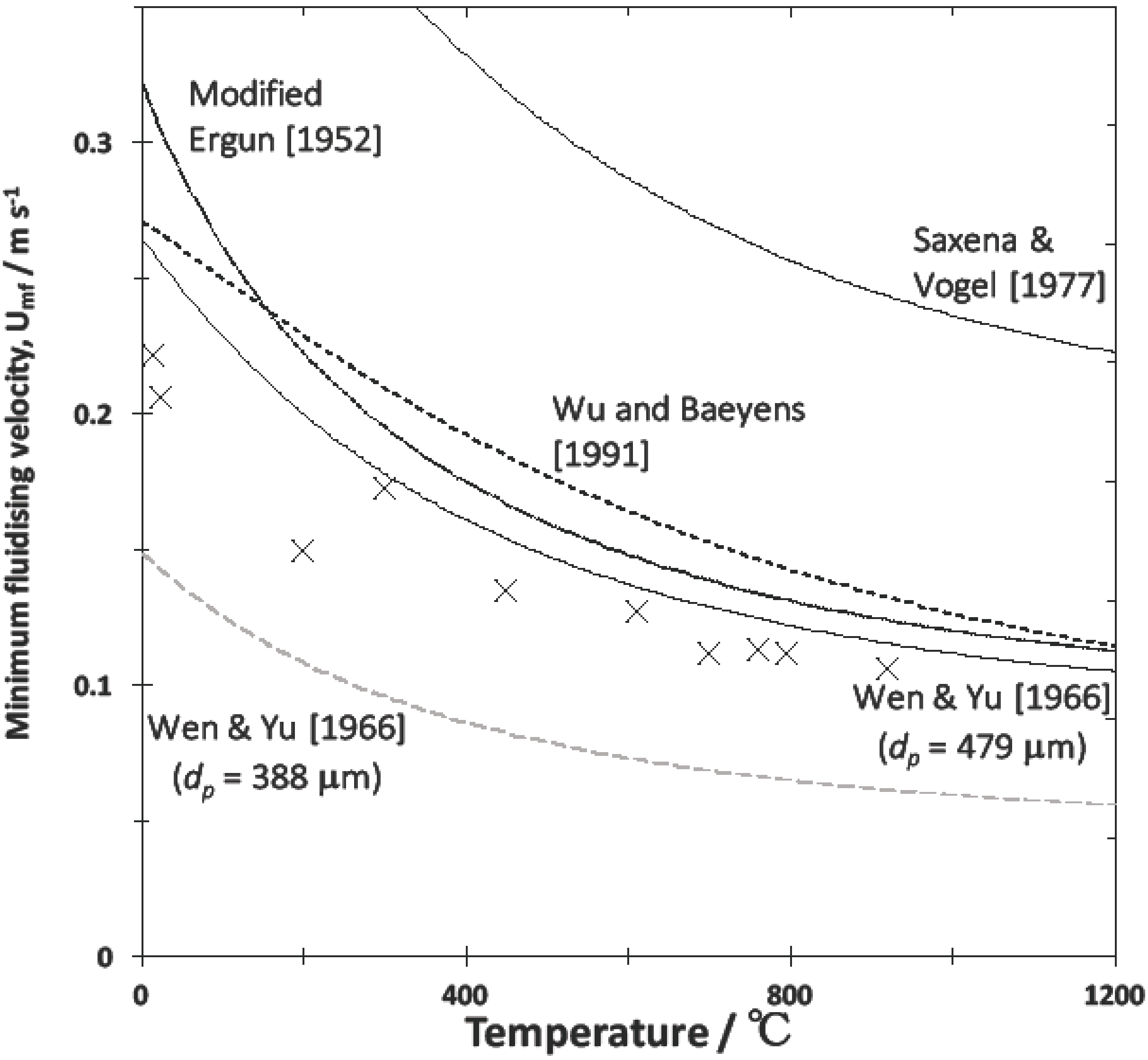

Fig. 8 - Comparison of the measured U_{mf} (X) with some correlations. The errors in the measured U_{mf} varied from ~ 3 % at high temperatures to ~ 8 % at room temperature; see the text. The curves labelled Wen and Yu [1966] used Eq. (8) and a particle size of either d_p = 0.388 mm (the geometric mean of the two sieve sizes) or d_p = 0.479 mm (the measured CE diameter). The modified Ergun Equation used Eq. (4) with d_p = 0.48 mm, ε_m = 0.45 and ϕ = 0.77 from Table 1. The curves labelled Saxena and Vogel [1977] and Wu and Baeyens [1991] are described in the text.

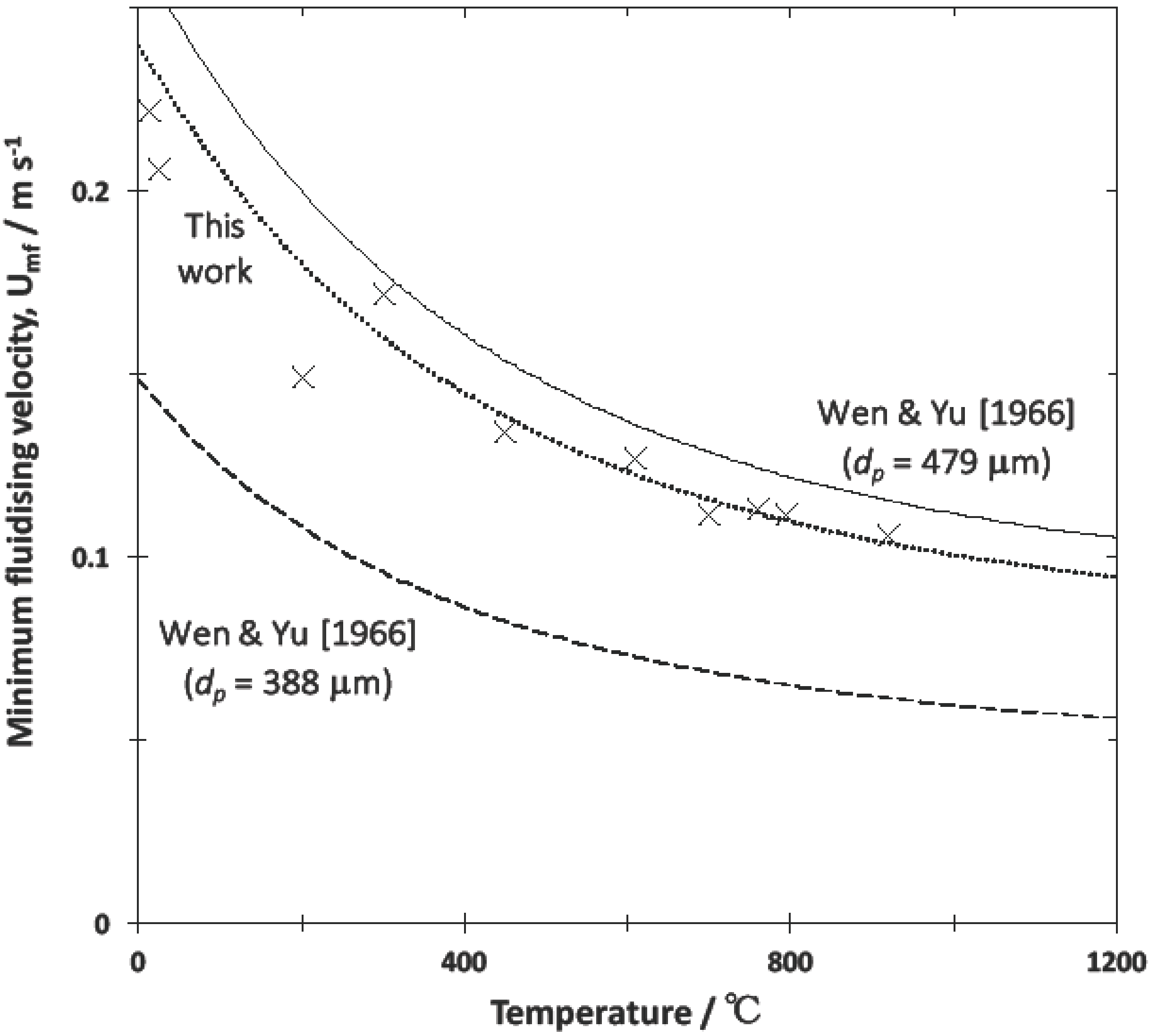

Fig. 9 - The measured U_{mf} (X), together with the two predictions (from Fig.8) of U_{mf} using Wen and Yu's correlation, Eq. (8) and two different sizes, d_p, for the particles. The finely dotted curve , labelled "This work" gives the new predictions using Ergun's Eq. (4) with Eq. (11) and the values of ϕ and d_p measured optically here.